

Characteristics of particulate-bound *n*-alkanes indicating sources of PM_{2.5} in Beijing, China

Jiyuan Yang¹, Guoyang Lei¹, Chang Liu¹, Yutong Wu¹, Kai Hu¹, Jinfeng Zhu¹, Junsong Bao², Weili Lin¹ and Jun Jin^{1,3}.

¹College of Life and Environmental Sciences, Minzu University of China, Beijing 100081, China

²State Key Laboratory of Water Environment Simulation, School of Environment, Beijing Normal University, Beijing, 100875, China

³Beijing Engineering Research Center of Food Environment and Public Health, Minzu University of China, Beijing 100081, China

Correspondence to: Jun Jin (junjin3799@126.com)

Abstract. The characteristics of *n*-alkanes and the contributions of various sources of fine particulate matter (PM_{2.5}) in the atmosphere in Beijing were investigated. PM_{2.5} samples were collected at Minzu University of China between November 2020 and October 2021, and *n*-alkanes in the samples were analyzed by gas chromatography-mass spectrometry. A positive matrix factorization analysis model and source indices (the main carbon peaks, carbon preference indices, and plant wax contribution ratios) were used to identify the sources of *n*-alkanes, determine the contributions of different sources, and explain the differences. The *n*-alkane concentrations were 4.51–153 ng/m³, (mean 32.7 ng/m³), and the particulate-bound *n*-alkane and PM_{2.5} concentrations varied in parallel. There were marked seasonal and diurnal differences in the *n*-alkane concentrations ($p < 0.01$). The *n*-alkane concentrations in the different seasons decreased in the order of winter > spring > summer > fall. The mean concentration of each homolog was higher at night than in the day in all seasons. Particulate-bound *n*-alkanes were supplied by common anthropogenic and biogenic sources, and fossil fuel combustion was the dominant contributor. The positive matrix factorization model results indicated five sources of *n*-alkanes in PM_{2.5}, which were coal combustion, diesel vehicle emissions, gasoline vehicle emissions, terrestrial plant release, and mixed sources. Vehicle emissions were the main sources of *n*-alkanes, contributing 57.6%. The sources of PM_{2.5} can be indicated by *n*-alkanes (i.e., using *n*-alkanes as organic tracers). Vehicle exhausts strongly affect PM_{2.5} pollution. Controlling vehicle exhaust emissions is key to controlling *n*-alkanes and PM_{2.5} pollution in Beijing.

1 Introduction

Serious air pollution in China is currently caused by a combination of haze and photochemical smog (Ma et al., 2012). The effects of haze on air quality are more obvious than the effects of photochemical pollution, which is relatively invisible. Haze is frequent in urban areas with relatively dense populations and high traffic loads. Fine particulate matter is the main pollutant involved in haze. Fine particulate matter has small particle sizes (aerodynamic equivalent diameter ≤ 2.5 microns), a long atmospheric retention time, and a complex chemical composition. Fine particulate matter is also a good substrate for chemical reactions, about which there is a great concern because the products can negatively affect the environment and human health (Wang et al., 2016; Zhu et al., 2005; Zhang, et al., 2015). In recent years, measures such as energy structure adjustments, pollutant emission controls, and air pollution prevention have markedly decreased atmospheric pollution and improved air quality in China. For example, the PM_{2.5} concentration in Beijing, a typical large city in China, has recently decreased markedly. The annual mean PM_{2.5} concentration decreased from 73 $\mu\text{g}/\text{m}^3$ in 2016 to 33 $\mu\text{g}/\text{m}^3$ (meeting the requirement of the secondary ambient air quality standard for China, 35 $\mu\text{g}/\text{m}^3$) in 2021 (Beijing Ecology and Environment Statement, 2016-2021). Sources of fine particulate matter need to be better understood and controlled to decrease PM_{2.5}

39 pollution, improve air quality, and meet the primary ambient air quality standard for China ($15 \mu\text{g}/\text{m}^3$) and even the World
40 Health Organization standard ($5 \mu\text{g}/\text{m}^3$).

41 It has been found that *n*-alkanes are important components of organic pollutants in particulate matter and are mainly supplied
42 through anthropogenic emissions such as vehicle exhausts, fossil fuel combustion, and biomass combustion (Liu et al., 2013)
43 or through biogenic emissions such as from microorganisms and terrestrial plants (Simoneit et al., 1989; Rogge et al., 1993).
44 *n*-Alkanes are non-polar saturated hydrocarbons that are stable and found at high concentrations in the atmosphere. *n*-
45 Alkanes readily adsorb to particles and can affect the environment and human health (Chen et al., 2019). *n*-Alkanes can
46 participate in atmospheric chemical reactions, and *n*-alkane volatility and reactivity decrease as the carbon chain length
47 increases (Aumont et al., 2013). The products of reactions involving short-chain *n*-alkanes ($C \leq 16$) in the environment
48 strongly contribute to the secondary organic aerosol formation (Michoud et al., 2012). Long-chain *n*-alkanes ($C > 16$) are
49 relatively stable in the environment and generally accumulate in particulate matter (Chrysikou et al., 2009). The carbon
50 number ranges, molecular compositions, and distributions of *n*-alkane mixtures in the particulate matter can be used to assess
51 aerosol migration and particulate matter sources. Particulate-bound *n*-alkanes play an important role in studying organic
52 aerosols and the sources of $\text{PM}_{2.5}$. The characteristics and sources of *n*-alkanes in the fine particulate matter are important
53 parameters for developing pollutant control strategies to sustainably decrease haze pollution and improve air quality.

54 Previous studies of *n*-alkanes in the atmospheric particulate matter have mainly been focused on concentrations (Wang et al.,
55 2005; Wang et al., 2006; Chen et al., 2014; Ren et al., 2017), characteristics (Simoneit et al., 2004; Li et al., 2013; Kang et al.,
56 2016), and sources (Kavouras et al., 2001; Bi et al., 2003; Fu et al., 2010; Sun et al., 2021). A wide range of *n*-alkanes is
57 present in the atmosphere, including highly and poorly volatile *n*-alkanes with carbon chain lengths between 8 and 40 (Kang
58 et al., 2016; Aumont et al., 2012). *n*-Alkane concentrations between tens and hundreds of nanograms per cubic meter have
59 been found in fine particles (Ren et al., 2016; Lyu et al., 2019). The *n*-alkane concentration is affected by factors such as
60 meteorological conditions and contributing sources and is related to the particulate matter concentration and particle size
61 distribution. The total *n*-alkane concentrations in particulate matter markedly vary by season, usually being higher in winter
62 and lowest in summer and fall (Lyu et al., 2016; Chen et al., 2019). *n*-Alkanes from different sources have different
63 molecular compositions and distributions that can be used to indicate the relative contributions of different sources of
64 particulate matter (Han et al., 2018).

65 In the past few decades, researchers in Zhengzhou (Wang et al., 2017), Guangzhou (Bi et al., 2003; Wang et al., 2016),
66 Shanghai (Lyu et al., 2016; Xu et al., 2015), Beijing (Ren et al., 2016; Lyu et al., 2019), Seoul (Kang et al., 2020), and Spain
67 (Caumo et al., 2020) have studied *n*-alkanes in atmospheric aerosols and determined total *n*-alkane concentrations, particle
68 size distributions, and the contributions of different sources. However, *n*-alkanes with different carbon number ranges were
69 analyzed in the different studies. Most studies were focused on *n*-alkanes containing < 30 carbon atoms, but these do not fully
70 reflect the sources of *n*-alkanes in particulate matter. Air quality in Beijing is gradually improving, and exploring strategies
71 for controlling sources of fine particulate matter further requires more information about *n*-alkane homolog distributions and
72 variability in fine particulate matter and the relative contributions of different sources. Beijing is a large city with a dense
73 population and high traffic volumes. The sources of *n*-alkanes and particulate matter in Beijing require attention because of
74 the large number of volatile organic pollutants present, the high levels of vehicle exhaust emissions, and relatively severe
75 particulate matter pollution. Secondary aerosols have been found to make strong contributions to particulate pollution during
76 haze episodes in urban areas (Presto et al., 2009; Huang et al., 2014). *n*-Alkanes only contribute a proportion of the total
77 organic matter in the particulate matter but are important contributors to particulate pollution by being important precursors
78 of secondary organic aerosols (Yang et al., 2019). *n*-Alkanes are also important indicators of the sources of particulate matter.
79 In this study, the concentrations of C_{13} – C_{40} *n*-alkanes in atmospheric fine particulate matter in Beijing between 2020 and
80 2021 were determined. Diurnal and seasonal variations in *n*-alkane homolog concentrations were assessed by performing the
81 diurnal and cross-seasonal sampling. The sources of *n*-alkanes were identified and the contributions of these sources to the

82 total *n*-alkane concentrations were determined using source indices and correlation models. The aim was to use *n*-alkanes to
83 indicate the sources of particulate matter to allow strategies for controlling particulate matter concentrations in urban areas to
84 be developed.

85 **2 Materials and methods**

86 **2.1 Sampling site and time**

87 Fine particulate matter samples were collected between November 2020 and October 2021 on the roof (about 20 m above the
88 ground) of the College of Pharmacy at the Minzu University of China (116.19° E, 39.57° N). Beijing is a typical heavily
89 populated and traffic-intensive Chinese city, with high emission intensities of nitrogen oxides and volatile organic pollutants
90 and relatively serious fine particulate matter pollution. Haidian District is a prosperous urban area in Beijing with intense
91 human activities and busy traffic. The sampling point in Haidian District reflected the influences of human activities and
92 vehicle emissions on fine particulate matter concentrations. Samples were collected between the 23rd and 29th of each
93 month during the study, but the exact sampling periods were adjusted to take into account pollution levels and the weather.
94 Samples were collected in two periods on a sampling day. Daytime samples were collected between 07:00 and 20:00 and
95 nighttime samples were collected between 20:30 and 06:30 the next morning. Diurnal and seasonal variations in *n*-alkane
96 concentrations in the fine particulate matter were investigated by collecting separate day and night samples and collecting
97 samples in different seasons. The effects of *n*-alkanes on PM_{2.5} concentrations were assessed by analyzing the correlation
98 between their concentrations.

99 **2.2 Sample collection and pretreatment**

100 Each fine particulate sample was collected using a TH-16A low-flow sampler (Wuhan Tianhong, Wuhan, China) containing
101 a Whatman QMA quartz fiber filter (Ø 47 mm; GE Healthcare Bio-Sciences, Pittsburgh, PA, USA) using a flow rate of 16.7
102 L/min. Before use, the quartz fiber filters were baked at 550 °C for 5 h to remove organic matter. Each filter was loosely
103 wrapped in aluminum foil and equilibrated for 24 h at 20 °C and 40% relative humidity and then weighed using a precision
104 electronic balance before being used to collect a sample. Once used, a filter was equilibrated for 24 h at 20 °C and 40%
105 relative humidity, weighed again, and then stored wrapped in aluminum foil at -20 °C.

106 The details for ultrasonic extraction methods used to analyze the samples of *n*-alkanes in PM_{2.5} are reported in previous
107 studies (Yang et al., 2019; Kang et al., 2020; Caumo et al., 2020). Each filter was cut into pieces and extracted by
108 ultrasonically with 15 mL of dichloromethane for 15 min. The extraction step was repeated five times, and the extracts
109 were combined and evaporated to 2 mL using a rotary evaporator. The extract was then transferred to a 15 mL centrifuge
110 tube and centrifuged at 3000 rpm for 5 min. The supernatant was evaporated just to dryness under a gentle flow of high-
111 purity nitrogen and then redissolved in 100 µL of toluene for instrumental analysis.

112 **2.3 Instrumental analysis**

113 The *n*-alkanes (C₁₃-C₄₀) were analyzed qualitatively and quantitatively by gas chromatography-mass spectrometry using an
114 Agilent 6890N-5975 system (Agilent Technologies, Santa Clara, CA, USA). *n*-Alkane standards (C₈-C₄₀) were purchased
115 from AccuStandard (New Haven, CT, USA). Separation was achieved using an Agilent J&W Scientific DB-5M column (30
116 m long, 0.25 mm inner diameter, 0.1 µm film thickness; Agilent Technologies). The temperature of the GC inlet was 290°C,
117 splitless injection mode was used, and the injection volume was 1.0 µL. The carrier gas was helium and the constant flow
118 rate was 1.0 mL/min. The oven temperature program started at 80 °C, which was held for 2 min, then increased at 10 °C/min
119 to 200 °C, and then increased at 15 °C/min to 300 °C, which was held for 30 min. The mass spectrometer was used in

120 electron impact ionization mode and selected ion detection mode. Ions with mass-to-charge ratios of 85 and 113
121 (characteristic of *n*-alkanes) were used to identify and quantify *n*-alkanes. The data were quantified using ChemStation
122 software (Agilent Technologies).

123 **2.4 Quantitative analysis**

124 Particulate-bound *n*-alkanes were quantified by an external standard method. We prepared standard solutions of C₈-C₄₀ *n*-
125 alkanes with concentration gradients of 10 ppm, 1 ppm, 500 ppb, 100 ppb, 50 ppb, and 10 ppb. The calibration curves were
126 plotted with the concentrations of the standard solution as the abscissa axis and the corresponding chromatographic response
127 obtained by GC-MS as the ordinate axis, the correlation coefficient of each calibration curve is greater than 0.99. The
128 concentrations of particulate-bound *n*-alkanes were finally quantified by the calibration curves.

129 **2.5 Quality assurance and control**

130 When extracting *n*-alkanes from the fine particulate samples, blank samples were extracted with each batch of samples. The
131 concentration of an analyte substance in the blanks was subtracted from the concentration of the analyte in a sample during
132 data processing. The detection and quantification limits of the instrument were defined as three and 10 times the signal-to-
133 noise ratio, respectively. The instrument detection limits for the *n*-alkanes were 1–10 pg.

134 A spiked recovery experiment was used to evaluate the recovery efficiency of particulate-bound *n*-alkanes. A mixed standard
135 solution of C₈-C₄₀ *n*-alkanes (20 μL, 1 ppm) was added to the blank samples, then the blank samples were pre-treated
136 according to the same methods and the concentrations of *n*-alkanes were detected by GC-MS. The recovery was calculated
137 based on the theoretical concentrations of *n*-alkanes standard solution and the measured concentrations of *n*-alkanes in the
138 blank spiked samples. The blank spiked recovery experiments were repeated three times and the final recovery was averaged
139 over the three experiments, the extraction recovery for *n*-alkanes range from 43.6% to 128%, and the RSD for the
140 concentrations of *n*-alkanes in the parallel samples of the blank spiked recovery experiments is 3.51%.

141 **2.6 Data analysis**

142 PM_{2.5} data were provided by the China Meteorological Administration (cma.gov.cn/). Data analysis (statistical and other
143 analyses of the *n*-alkane data) was performed using SPSS 26.0 software (IBM, Armonk, NY, USA). Differences in the
144 concentrations of an *n*-alkane homolog in different groups of samples and differences in the overall *n*-alkane compositions in
145 different groups of samples were assessed by performing independent sample t-tests. Spearman correlations and Pearson
146 correlations (two-tailed tests) were used to identifying correlations between groups of data.

147 Source indices (the carbon maximum number (C_{max}), carbon preference index (CPI), and plant wax *n*-alkane ratio
148 (WNA%)) were used to assess the *n*-alkane sources from the *n*-alkane molecular compositions and concentration
149 distributions. The C_{max} is the homolog with the highest relative concentration in the *n*-alkane mixture, it is commonly used
150 to distinguish between the contributions of anthropogenic and natural sources of *n*-alkanes and is related to the degree of
151 thermal evolution that has affected the organic matter supplying *n*-alkanes. The CPI was defined as the ratio of total odd
152 carbon *n*-alkanes to even carbon *n*-alkanes and was developed by Bray and Evans in 1961 (Bray et al., 1961), it can be used
153 to assess the contributions of anthropogenic and biogenic sources of *n*-alkanes and is the most commonly used empirical
154 parameter for distinguishing between sources of *n*-alkanes (Marzi et al., 1993). WNA% and PNA% (petrogenic *n*-alkane
155 ratio) can be used to assess the relative contributions of biological and anthropogenic sources of *n*-alkanes in particulate
156 matter (Simoneit, 1985), WNA% are calculated by subtraction of the average of the next higher and lower even carbon
157 numbered homologs, while PNA% was defined as the WNA% subtracted from 100% (Lyu et al., 2019). The source indices
158 were calculated using Eqs. (1)–(3):

$$159 \quad \text{CPI} = \frac{\sum_{i=6}^{19} C_{2i+1}}{\sum_{i=7}^{20} C_{2i}} \quad (1)$$

$$160 \quad \text{WNA}\% = \frac{\sum (C_n - (\frac{C_{n-1} + C_{n+1}}{2}))}{\sum C_n} \times 100\% \quad (\text{"n" is an odd number}) \quad (2)$$

$$161 \quad \text{PNA}\% = 100\% - \text{WNA}\% \quad (3)$$

162 In Eq. (1), C_{2i+1} was the concentration of the n -alkane with odd carbon atoms ranging from 13-39, while C_{2i} was the
 163 concentration of the n -alkane with even carbon atoms ranging from 14-40. In Eq. (2), C_n was the concentration of n -alkanes,
 164 taking as zero the negative value of $(C_n - (\frac{C_{n-1} + C_{n+1}}{2}))$.

165 A positive matrix factorization (PMF) model was used to identify specific n -alkane sources and the contribution of each
 166 source through EPA PMF 5.0 software (USEPA). The PMF model is a factor analysis technique using multivariate statistical
 167 methods. The PMF model is a receptor model, so can identify and determine the contributions of components of unknown
 168 mixtures. The PMF model is one of the source resolution methods recommended by the US Environmental Protection
 169 Agency. The PMF model does not require the complex pollutant sources to be determined beforehand and the treatment
 170 process can be optimized while limiting the decomposition matrix elements and sharing the rates of nonnegative matrices.
 171 The model can use the chemical composition of particulate matter to identify the sources of particulate matter and calculate
 172 the contributions of the different sources, so is widely used to investigate the sources of atmospheric particulate matter
 173 (Moeinaddini et al., 2014; Liao et al., 2021; Li et al., 2021). The details of PMF have been described in the PMF 5.0 User
 174 Guide (USEPA, 2014).

175 **3 Results**

176 **3.1 Concentrations of n -alkanes**

177 A total of 28 n -alkane homologs with carbon chain lengths of C_{13} – C_{40} were analyzed. C_{13} – C_{40} n -alkanes were detected in the
 178 diurnal fine particulate matter samples collected in all seasons. Among them, C_{21} – C_{35} n -alkanes were detected in all $\text{PM}_{2.5}$
 179 samples, and other n -alkanes were detected in more than half of the samples.

180 The n -alkane and $\text{PM}_{2.5}$ concentrations in the different seasons are shown in Table 1 and temporal variations in the average
 181 concentrations between day and night are shown in Figure 1. The $\text{PM}_{2.5}$ concentrations throughout the sampling period were
 182 0–134 $\mu\text{g}/\text{m}^3$, and the mean was 32.0 $\mu\text{g}/\text{m}^3$. The n -alkane concentrations throughout the sampling period were 4.51–153
 183 ng/m^3 , and the mean was 32.7 ng/m^3 . As shown in Figure 2, under the condition of excluding the influence of the sharp rise
 184 of $\text{PM}_{2.5}$ concentration in heavy haze days, correlation analysis indicated that the n -alkane and $\text{PM}_{2.5}$ concentrations
 185 significantly positively correlated ($p < 0.01$, $r = 0.618$).

186 **3.2 n -Alkane component distributions**

187 The contributions of the individual C_{13} – C_{40} n -alkane homologs to the total n -alkane concentrations are shown in Figure 3.
 188 The C_{16} – C_{25} n -alkanes were dominant in winter and the C_{26} – C_{31} n -alkane contributions increased markedly in spring,
 189 summer, and fall.

190 The n -alkane homologs can be classed as low molecular weight (LMW), meaning n -alkanes with carbon chain lengths ≤ 25 ,
 191 and high molecular weight (HMW), meaning n -alkanes with carbon chain lengths > 25 . As shown in Figure 4, LMW n -
 192 alkanes contributed $\sim 60\%$ of the total n -alkane concentrations in winter but only $\sim 40\%$ in spring, summer, and fall,
 193 indicating that there were marked differences between the compositions in winter and the other seasons.

194 3.3 Seasonal and diurnal differences in *n*-alkane concentrations

195 The average concentration distributions of C₁₃–C₄₀ *n*-alkanes in the different seasons are shown in Figure 5. There were
196 significant differences ($p < 0.01$) between the concentrations of various homologs in the different seasons. The mean *n*-alkane
197 concentrations for the different seasons decreased in the order of winter > spring > summer > fall. The seasonal differences were
198 more marked for LMW than HMW *n*-alkanes. The concentrations of relatively short-chain *n*-alkanes (C₁₆–C₂₅) were
199 markedly higher in winter than in the other seasons. The concentrations of C₂₇, C₂₉, C₃₁, and C₃₃ *n*-alkanes were higher than
200 the concentrations of C₂₆, C₂₈, C₃₀, C₃₂, and C₃₄ *n*-alkanes (i.e., odd-carbon-number dominance occurred) in all of the seasons.
201 The C₁₃–C₄₀ *n*-alkane concentrations in the day and night samples are shown in Figure 6. The mean *n*-alkane homolog
202 concentrations were higher at night than during the day in all four seasons. The concentrations during the day and night were
203 significantly different ($p < 0.01$). Statistical tests on the differences in concentration of individual homologs of *n*-alkanes
204 between day and night in different seasons showed that fewer *n*-alkane homologs with significant differences in winter (C₁₆,
205 C₁₇) and spring (C₂₁) while more *n*-alkane homologs ($C > 21$) with significant differences in summer and autumn.

206 3.4 Source indices and PMF model

207 Source indices (C_{max}, CPI, and WNA%) determined from the C₁₃–C₄₀ *n*-alkane data were used to assess the *n*-alkane
208 sources. The PMF model was used to quantify the amounts of *n*-alkanes in fine particles supplied by the different sources
209 and the relative contributions of the sources. The source index data for *n*-alkanes in the day and night samples in the different
210 seasons are shown in Table 2.

211 3.4.1 Source indices for *n*-alkanes

212 The C_{max} for winter was C₂₃ but the C_{max} for spring, summer, and fall was C₂₉. The mean CPI for the year the samples
213 were collected was 1.66. The CPI was lowest in winter but higher during the day than the night in spring, summer, and fall.
214 The mean contribution of plant wax *n*-alkanes to the total *n*-alkane concentration during the sampling period was 30.6% and
215 the mean contribution of anthropogenic *n*-alkanes to the total *n*-alkane concentration was 69.4%. The plant wax *n*-alkane
216 contribution was lowest in winter and markedly higher in spring, summer, and fall.

217 3.4.2 Results of the PMF model

218 According to the PMF 5.0 User Guide (USEPA, 2014), the daily mean *n*-alkane concentrations during the sampling period
219 and the corresponding uncertainties were inputted into the PMF model to analyze the sources of *n*-alkanes in fine particulate
220 matter. Various numbers of factors were tested, and the optimal correlation coefficient for the relationship between the
221 simulated and observed values was found when five factors were used, the average correlation coefficient of *n*-alkane
222 homologs is 0.832. Q (robust) is an important parameter obtained after PMF run, it is the goodness-of-fit parameter
223 calculated excluding points not fit by the model (USEPA, 2014). In the process of running the PMF model, we got the lowest
224 Q (robust) values when selecting five factors. This met the requirements to use the PMF model, EPA PMF 5.0 User Guide
225 (USEPA, 2014) has stated that the lowest Q (robust) value represents the most optimal solution from the multiple runs and it
226 can be a critical parameter for choosing the optimal number of factors. Each factor indicated a source, and the factors could
227 be used to identify the corresponding sources. The *n*-alkane factor data given by the PMF model are shown in Figure 7.
228 The PMF model indicated that the contributions of factors 1, 2, 3, 4, and 5 to the *n*-alkane concentrations were 14.8%, 26.1%,
229 31.5%, 18.6%, and 9.01%, respectively. The sources corresponding to the factors identified by the PMF model needed to be
230 identified from the proportions of the different *n*-alkane homologs present, the sources corresponding to factors 2 and 3 were
231 the main contributors of *n*-alkanes in particulate matter.

233 4.1 Sources and contributions of *n*-alkanes

234 *n*-Alkanes in PM_{2.5} have relatively complex sources, but different *n*-alkane compositions and distributions indicate different
235 sources. As shown in Figure 5, marked odd-carbon-number dominance was found in all seasons for the HMW *n*-alkanes,
236 with *n*-alkanes with carbon chain lengths C₂₇, C₂₉, C₃₁, and C₃₃ being dominant. No odd-carbon-number dominance was
237 found for the LMW *n*-alkanes. It has previously been found that LMW *n*-alkanes in urban areas are mainly anthropogenic
238 (e.g., emitted during fossil fuel combustion and in vehicle exhaust gases) (Simoneit et al., 2004; Kang et al., 2016) but HMW
239 *n*-alkanes reflect sources such as biomass combustion and waxes in terrestrial plants (Kawamura et al., 2003). LMW and
240 HMW *n*-alkane patterns can be used to identify the main sources of *n*-alkanes in urban areas. The *n*-alkane patterns in the
241 different seasons indicated that particulate-bound *n*-alkanes in the atmosphere in Beijing have both anthropogenic and
242 biological sources. The source indices and PMF model results further explained the sources and contributions of *n*-alkanes.

243 *n*-Alkane source indices are often used to identify the origins of *n*-alkanes. The *n*-alkane source indices shown in Table 2
244 indicated that anthropogenic emissions were the main contributors of particulate-bound *n*-alkanes in Beijing during the study
245 but that there were also biogenic emissions of particulate-bound *n*-alkanes. The CPI and WNA% data explained this. During
246 the sampling period, the mean CPI was 1.66, indicating that the main sources of particulate-bound *n*-alkanes were fossil fuel
247 combustion, plants, and biomass combustion. The mean WNA% and PNA% were 30.63% and 69.37%, respectively,
248 indicating that anthropogenic emissions contributed more than emissions from biota.

249 The PMF model can quantify the contributions of specific sources of *n*-alkanes relatively accurately. The *n*-alkane homolog
250 contributions to each factor identified by the PMF model were used to analyze and identify the corresponding source. As
251 shown in factor 1 of Figure 7, the *n*-alkanes with carbon chain lengths of C₁₃–C₁₈ were dominant, which is similar to the *n*-
252 alkane homolog (C<20) pattern for emissions during coal combustion found by Oros and Simoneit and Niu et al. (Oros et al.,
253 2000; Niu et al., 2005). Therefore, we concluded that factor 1 indicated *n*-alkanes emitted through coal combustion. Vehicle
254 emissions are important sources of *n*-alkanes in particulate matter in urban areas (Lyu et al., 2019). *n*-Alkanes emitted by
255 vehicles mainly have carbon-chain lengths <30 (Wang et al., 2017). However, there are marked differences between the
256 patterns of *n*-alkanes emitted in particulates in gasoline vehicles and diesel vehicle exhaust gases. C_{max} for *n*-alkanes is
257 lower and the proportion of low-carbon-chain length *n*-alkanes is higher for particulates in diesel vehicle exhaust gases than
258 gasoline vehicle exhaust gases. This feature can be used to distinguish between *n*-alkanes emitted by diesel and gasoline
259 vehicles in fine particulate matter (Fujitani et al., 2012; Yuan et al., 2016). As shown in Figure 7, the homologs with a higher
260 proportion of *n*-alkane species in factor 2 are concentrated around C₂₀, while in factor 3 are concentrated around C₂₇.
261 According to studies by Sachuer et al. for gasoline and diesel vehicle emissions (Schauer et al., 1999; Schauer et al., 2002),
262 we determine that factor 2 and factor 3 indicated diesel and gasoline vehicle emission sources, respectively. C₂₇–C₃₈ (i.e.,
263 high-carbon-chain-length) *n*-alkanes made large contributions and low-carbon-chain-length *n*-alkanes made small
264 contributions to the pattern for factor 4. Studies have shown that C₂₆–C₃₆ *n*-alkanes are mainly emitted from cuticular waxes
265 in terrestrial plants (Alves et al., 2001; Lyu et al., 2016), so we inferred that factor 4 indicated *n*-alkanes emitted by terrestrial
266 plants. *n*-Alkanes do not have an obvious regularity in composition and there was no clear *n*-alkane homologs pattern for
267 factor 5, but long-chain *n*-alkanes with carbon chain lengths ≥34 were dominant. We found that road dust is one of the
268 sources of particulate-bound *n*-alkanes (Anh et al., 2019), *n*-alkanes with ≥C₃₄ may come from road dust (Daher et al., 2013)
269 and biogenic source (Liebezeit et al., 2009). Therefore, we concluded that factor 5 may be the mixed sources of *n*-alkanes
270 from road dust and biogenic emissions.

271 The contributions of the different sources to the *n*-alkane concentrations are shown in Figure 8. In summary, *n*-alkanes in
272 airborne particulate matter in Beijing are both anthropogenic and biogenic. Vehicle exhaust emissions are the main sources
273 of *n*-alkanes, consistent with the current energy consumption structure in Beijing, and gasoline and diesel vehicles accounted

274 for a relatively large proportion of *n*-alkanes in airborne particulate matter.

275 **4.2 Characteristics of PM_{2.5} and *n*-alkanes**

276 The mean *n*-alkane concentration during the sampling period was 32.7 ng/m³, which was lower than the C₁₉–C₃₆ *n*-alkane
277 concentration of 282 ng/m³ found in Beijing in 2006 (Li et al., 2013) and the C₈–C₄₀ *n*-alkane concentration of 228 ng/m³
278 found in Shanghai in 2013 (Lyu et al., 2016). The temporal trends in the *n*-alkane concentrations were similar to the trends
279 found in previous studies of *n*-alkanes in Beijing (Rogge et al., 1993; Li et al., 2013; Ren et al., 2019), the overall *n*-alkane
280 concentration being highest in winter. The seasonal pattern we found for *n*-alkanes in Beijing was similar to the pattern
281 found in a previous study of C₁₆–C₃₅ *n*-alkanes in 14 Chinese cities (Wang et al., 2006).

282 The *n*-alkane pattern varied by season, with LMW *n*-alkanes being dominant in winter and HMW *n*-alkanes being more
283 abundant in the other seasons. C_{max} and WNA% explained the seasonal differences in the *n*-alkane patterns. In previous
284 studies, lower C_{max} values were found for *n*-alkanes emitted from very mature organic matter such as coal and petroleum
285 than for *n*-alkanes emitted from immature organic matter such as plants (Simoneit et al., 1989; Duan et al., 2010). The C_{max}
286 for *n*-alkanes in winter was C₂₃, indicating that LMW *n*-alkanes were the main *n*-alkanes. Similar results were found by Lyu
287 et al. for Beijing in winter (Lyu et al., 2019). The C_{max} for *n*-alkanes in spring, summer, and fall was C₂₉. Ficken et al.
288 (Ficken et al., 2000) and Yadav et al. (Yadav et al., 2013) found that C₂₉ *n*-alkanes are markers for *n*-alkanes emitted from the
289 wax layers of terrestrial plants. Stronger *n*-alkane contributions will be made by plants in spring, summer, and fall than in
290 winter (Rogge et al., 1993; Yadav et al., 2013). This is consistent with the results found in a study performed in Shanghai
291 (Lyu et al., 2016; Wang et al., 2016). There were significant seasonal differences (p<0.01) in the concentrations of the C₁₃–
292 C₄₀ *n*-alkane homologs, but the seasonal differences were stronger for LMW *n*-alkanes than HMW *n*-alkanes. Similar results
293 were found by Li et al. in Tianjin in 2010 (Li et al., 2010). The LMW *n*-alkane concentrations were markedly higher in
294 winter than in the other seasons, similar to the results of a study performed by Li et al. in Beijing in 2013 (Li et al., 2013).
295 This indicated that there were seasonal differences in *n*-alkane sources. The PMF model results shown in Figure 8 indicated
296 that anthropogenic *n*-alkanes strongly contributed to the total *n*-alkane concentration in winter. The CPI also indicated that
297 different sources were dominant in winter and the other seasons. The lowest CPI was found for winter, indicating that LMW
298 *n*-alkanes made stronger contributions to the total *n*-alkane concentrations in winter than in the other seasons. This may be
299 related to *n*-alkane emissions caused by fossil fuel combustion for heating in winter. Similar results have been found in
300 Shanghai (Lyu et al., 2016), Zhengzhou (Wang et al., 2017), southeastern Chinese cities (Chen et al., 2019), and Beijing
301 (Kang et al., 2016).

302 Meteorological factors affect the concentrations and composition of *n*-alkanes in different seasons. The mixing layer height
303 influences the concentration of *n*-alkanes by affecting the particulate matter, it's shown that the mixing layer height is
304 correlated with the concentration of particulate matter and the peak concentration of particulate matter increases as the
305 mixing layer height decreases (Wagner et al., 2017). The atmospheric mixing layer height in Beijing has obvious seasonal
306 characteristics, showing low in winter and high in summer (Wang et al., 2020; Tang et al., 2016). Therefore, the increased
307 concentrations of PM_{2.5} and *n*-alkanes in winter were influenced by the mixing layer height. Wind direction is one of the
308 factors affecting the seasonal differences in particulate matter and *n*-alkanes, the northwest wind in winter brought the
309 polluted air masses from inland to Beijing, while the southeast wind in summer transported cleaner aerosols from oceans to
310 here (Wei et al., 2020). In addition, the seasonal distribution of *n*-alkanes is influenced by the temperature. The temperature
311 in Beijing is high in summer and low in winter, when the temperature is lower in winter, gaseous *n*-alkanes are more likely to
312 partition into particles with the higher partition coefficient of gas-particle partitioning (Lyu et al., 2016; Wick et al., 2002).
313 Therefore, the increase of LWM *n*-alkanes proportion in winter is also affected by temperature.

314 The mean C₁₃–C₄₀ *n*-alkane homolog concentrations were higher at night than in the day in each season, and the differences

315 were significant ($p < 0.01$). According to a study by Yao et al. in 2009, lower average wind speeds, atmospheric mixing layer
316 height, and poorer atmospheric diffusion conditions can lead to higher concentrations of *n*-alkanes at night than during the
317 day (Yao et al., 2009). Similar results were found in Liaocheng, Shandong Province (Liu et al., 2019). The differences in the
318 *n*-alkane concentrations in the night and day may also have been caused by differences in pollutant emissions in the night
319 and day. Particulate-bound *n*-alkanes from vehicular emissions are usually of low molecular weight (Lyu et al., 2019), and
320 diesel emissions have higher concentrations of particulate-bound *n*-alkanes with carbon chain lengths less than 25 (Schauer
321 et al., 1999). Differences in diurnal concentrations of LMW *n*-alkanes may reflect the differences in the contribution of
322 anthropogenic sources. We found markedly higher concentrations of some homologs with carbon chain lengths < 25 at night
323 than during the day. This would be consistent with short-chain alkane emissions from diesel vehicles in Beijing being higher
324 at night than during the day.

325 **4.3 PM_{2.5} sources in Beijing and strategies for controlling PM_{2.5} concentrations**

326 During the sampling period, the mean daily PM_{2.5} concentration in Beijing was 32.0 $\mu\text{g}/\text{m}^3$, which met the requirement of the
327 secondary ambient air quality standard for China (35.0 $\mu\text{g}/\text{m}^3$). According to the Ecology and Environment Statement from
328 the Beijing Municipal Ecology and Environment Bureau (sthjj.beijing.gov.cn), the annual mean PM_{2.5} concentration in
329 Beijing has gradually decreased in the last five years. However, little research on *n*-alkanes in Beijing has been performed
330 during this period. We compared our results with the results of a previous study (Lyu et al., 2019) and found that the *n*-alkane
331 concentrations decreased in parallel with the PM_{2.5} concentrations. *n*-Alkanes are important molecular markers for
332 identifying the sources of PM_{2.5}. Excluding when the PM_{2.5} concentration increased sharply because of meteorological
333 conditions, the PM_{2.5} and *n*-alkane concentrations varied in the same ways. As shown in Figure 2, a significant positive
334 correlation was found between the PM_{2.5} and *n*-alkane concentrations ($p < 0.01$), so *n*-alkanes could be used as indicators of
335 the sources of PM_{2.5} in the atmosphere. This method has been widely used to analyze sources of particulate matter (Cass,
336 1998; Kavouras et al., 2001; Bi et al., 2003; Xu et al., 2013; Zhao et al., 2016; Han et al., 2018). Therefore, we used the PMF
337 model results for *n*-alkanes to identify the sources of PM_{2.5} and explain variations in the sources.

338 The PMF model results for the contributions of the different sources shown in Figure 8 indicated that emissions in vehicle
339 exhaust gases and through coal combustion contributed up to 72.4% of PM_{2.5} in the sampling area throughout the sampling
340 period. This indicated that anthropogenic PM_{2.5} emissions are the main sources of PM_{2.5} in the urban study area. Emissions
341 from gasoline and diesel vehicles were the dominant anthropogenic sources, contributing 57.6% of total anthropogenic PM_{2.5}
342 emissions. Vehicles are the main sources of PM_{2.5} in urban areas and make important contributions to particulate matter in
343 the atmosphere in Beijing. Similar results were found in a previous study of PM_{2.5} sources in Beijing (Lv et al., 2020; Qi et
344 al., 2018) and the results were consistent with the current energy consumption structure in Beijing (gasoline and diesel fuel
345 make large contributions to total fuel consumption). Human activities make larger contributions to PM_{2.5} emissions in winter
346 than in the other seasons, indicating that more attention should be paid to emissions caused by fossil fuel combustion in
347 winter than in the other seasons.

348 It is necessary to improve air quality in Beijing, and vehicle exhausts are key sources of PM_{2.5}. Further improvements in
349 ambient air quality to meet stricter ambient air quality standards will require vehicle emissions to be controlled to decrease
350 particulate matter pollution. The number of vehicles using fossil fuels in Beijing needs to be decreased. Achieving this will
351 require policies for restricting the use of vehicles using fossil fuels and the use of cleaner energy vehicles to be promoted. In
352 summary, controlling and decreasing emissions caused by fossil fuel combustion will decrease PM_{2.5} emissions and improve
353 ambient air quality in Beijing.

354 **5 Conclusions**

355 The PM_{2.5} concentrations and C₁₃–C₄₀ *n*-alkane concentrations in the fine particulate matter between November 2020 and
356 October 2021 were determined and the concentrations were compared with concentrations found in previous studies. The
357 PM_{2.5} and *n*-alkane concentrations in Beijing have decreased in similar ways in the last five years. The mean PM_{2.5}
358 concentration was 32.0 µg/m³, which met the secondary ambient air quality standard for China. The PM_{2.5} and C₁₃–C₄₀ *n*-
359 alkane concentrations varied in similar ways and positively correlated ($p < 0.01$), so long-chain *n*-alkanes in the particulate
360 matter can be used to assess the sources of particulate matter pollution in urban areas and to develop strategies for
361 controlling particulate matter pollution.

362 The *n*-alkane concentrations in the different seasons decreased in the order of winter>spring>summer>fall. There were
363 marked seasonal and diurnal differences in the *n*-alkane homolog patterns and distributions. The source indices and PMF
364 model results explained these variations in patterns and allowed the sources of *n*-alkanes to be identified. The source indices
365 indicated that *n*-alkane concentrations in particulate matter in Beijing are affected by both anthropogenic and biogenic
366 emissions but that anthropogenic emissions are dominant. The PMF model allowed the contributions of the sources of *n*-
367 alkanes to be quantified and indicated that emissions from vehicles are currently the main sources of PM_{2.5} and *n*-alkanes in
368 particulate matter in urban areas.

369 Controlling PM_{2.5} and *n*-alkanes emissions from vehicles is key to decreasing PM_{2.5} and *n*-alkanes pollution and improving
370 air quality in urban areas. *n*-Alkanes in the particulate matter can be used as organic tracers, and PMF model results can
371 indicate the sources of PM_{2.5} pollution. Further research into the use of this method is required.

372 **Acknowledgements**

373 This work was supported by the National Natural Science Foundation of China [grant no. 91744206] and the Beijing Science
374 and Technology Planning Project [Z181100005418016]. We also thank Dr. Gareth Thomas for his help in the grammatical
375 editing of this paper.

376 **Data availability**

377 The data presented in this article is available from the authors upon request (junjin3799@126.com).

378 **Author contribution**

379 JJ conceived and designed the study, provided direct funding, and helped with manuscript revision. JYY mainly conducted
380 the sampling, and sample analysis work, as well as manuscript writing and revision. Other authors helped this work by
381 sampling and analysis. All authors read and approved the final manuscript.

382 **Competing interests**

383 The authors declare that they have no conflict of interest.

384 **References**

385 Alves, C., Pio, C., and Duarte, A.: Composition of extractable organic matter of air particles from rural and urban Portuguese

386 areas, *Atmos. Environ.*, 35, 5485-5496, doi: 10.1016/S1352-2310(01)00243-6, 2001.

387 Aumont, B., Valorso, R., Mouchel-Vallon, C., Camredon, M., Lee-Taylor, J., and Madronich, S.: Modeling SOA formation
388 from the oxidation of intermediate volatility n-alkanes, *Atmos. Chem. Phys.*, 12, 7577-7589, doi: 10.5194/acp-12-7577-2012,
389 2012.

390 Aumont, B., Camredon, M., Mouchel-Vallon, C., La, S., Ouzebidour, F., Valorso, R., Lee-Taylor, J., and Madronich, S.:
391 Modeling the influence of alkane molecular structure on secondary organic aerosol formation, *Faraday Discuss.*, 165, 105-
392 122, doi: 10.1039/C3FD00029J, 2013.

393 Beijing Ecology and Environment Statement. sthjj.beijing.gov.cn, Beijing Municipal Ecology and Environmental Bureau,
394 2016-2021.

395 Bi, X. H., Sheng, G. Y., Peng, P. A. Chen, Y. J., Zhang, Z. Q., and Fu, J. M.: Distribution of particulate- and vapor-phase n-
396 alkanes and polycyclic aromatic hydrocarbons in urban atmosphere of Guangzhou, China, *Atmos. Environ.*, 37, 289-298, doi:
397 10.1016/S1352-2310(02)00832-4, 2003.

398 Bray, E. E., and Evans, E. D.: Distribution of n-paraffins as a clue to recognition of source beds, *Geochim. Cosmochim.*
399 *Acta.*, 22, 2-15, doi: 10.1016/0016-7037(61)90069-2, 1961.

400 Cass, G. R.: Organic molecular tracers for particulate air pollution sources, *Trends Analyt. Chem.*, 17, 356-366, doi:
401 10.1016/S0165-9936(98)00040-5, 1998.

402 Caumo, S., Bruns, R. E., and Vasconcellos, P. C.: Variation of the Distribution of Atmospheric n-Alkanes Emitted by
403 Different Fuels' Combustion, *Atmosphere*, 11, 643, doi: 10.3390/atmos11060643, 2020.

404 Chen, Q., Chen, Y., Luo, X. S., Hong, Y. W., Hong, Z. Y., Zhao, Z., and Chen, J. S.: Seasonal characteristics and health risks
405 of PM_{2.5}-bound organic pollutants in industrial and urban areas of a China megacity, *J. Environ. Manage.*, 245, 273-281, doi:
406 10.1016/j.jenvman.2019.05.061, 2019.

407 Chen, Y., Cao, J. J., Zhao, J., Xu, H. M., Arimoto, R., Wang, G. H., Han, Y. M., Shen, Z. X., and Li, G. H.: n-Alkanes and
408 polycyclic aromatic hydrocarbons in total suspended particulates from the southeastern Tibetan Plateau: concentrations,
409 seasonal variations, and sources, *Sci. Total Environ.*, 470-471, 9-18, doi: 10.1016/j.scitotenv.2013.09.033, 2014.

410 Chrysikou, L. P., and Samara, C. A.: Seasonal variation of the size distribution of urban particulate matter and associated
411 organic pollutants in the ambient air, *Atmospheric Environ.*, 43, 4557-4569, doi: 10.1016/j.atmosenv.2009.06.033, 2009.

412 Duan, F. K., He, K. B., and Liu, X. D.: Characteristics and source identification of fine particulate n-alkanes in Beijing,
413 China, *J. Environ. Sci. (in Chinese)*, 22, 998-1005, doi: 10.1016/S1001-0742(09)60210-2, 2010.

414 Ficken, K. J., Li, B., Swain, D. L., and Eglinton, G.: An n-alkane proxy for the sedimentary input of submerged/floating
415 freshwater aquatic macrophytes, *Org. Geochem.*, 31, 745-749, [https://doi.org/10.1016/S0146-6380\(00\)00081-4](https://doi.org/10.1016/S0146-6380(00)00081-4), 2000.

416 Fu, P. Q., Kawamura, K., Pavuluri, C. M., Swaminathan, T., and Chen, J.: Molecular characterization of urban organic
417 aerosol in tropical India: contributions of primary emissions and secondary photooxidation, *Atmos. Chem. Phys.*, 10, 2663-
418 2689, doi: 10.5194/acp-10-2663-2010, 2010.

419 Fujitani, Y., Saitoh, K., Fushimi, A., Takahashi, K., Hasegawa, S., Tanabe, K., Kobayashi, S., Furuyama, A., Hirano, S., and
420 Takami, A.: Effect of isothermal dilution on emission factors of organic carbon and n-alkanes in the particle and gas phases
421 of diesel exhaust, *Atmos. Environ.*, 59, 389-397, doi: 10.1016/j.atmosenv.2012.06.010, 2012.

422 Han, D. M., Fu, Q. Y., Gao, S., Li, L., Ma, Y. G., Qiao, L. P., Xu, H., Liang, S., Cheng, P. F., Chen, X. J., Zhou, Y., Yu, J. Z.,
423 and Chen, J. P.: Non-polar organic compounds in autumn and winter aerosols in a typical city of eastern China: size
424 distribution and impact of gas-particle partitioning on PM_{2.5} source apportionment, *Atmos. Chem. Phys.*, 18, 9375-9391, doi:
425 10.5194/acp-18-9375-2018, 2018.

426 Huang, R. J., Zhang, Y. L., Bozzetti, C., Ho, K. F., Cao, J. J., Han, Y. M., Daellenbach, R. K., Slowik, J. G., Platt, S. M.,
427 Canonaco, F., Zotter, P., Wolf, R., Pieber, S. M., Bruns, E. A., Crippa, M., Ciarelli, G., Piazzalunga, A., Schwikowski, M.,
428 Abbaszade, G., Schnelle-Kreis, J., Zimmermann, R., An, Z. S., Szidat, S., Baltensperger, U., Haddad, I. E., and Prévôt, A. S

429 H: High secondary aerosol contribution to particulate pollution during haze events in China, *Nature*, 514, 218-222, doi:
430 10.1038/nature13774, 2014.

431 Kang, M. J., Fu P. Q., Aggarwal, S. G, Kumar, S., Zhao, Y., Sun, Y. L., and Wang, Z. F.: Size distributions of n-alkanes, fatty
432 acids and fatty alcohols in springtime aerosols from New Delhi, India, *Environ. Pollut.*, 219, 957-966, doi:
433 10.1016/j.envpol.2016.09.077, 2016.

434 Kang, M. J., Ren, L. J., Ren, H., Zhao, Y., Kawamura, K., Zhang, H. L., Wei, L. F., Sun, Y. L., Wang, Z. F., and Fu, P. Q.:
435 Primary biogenic and anthropogenic sources of organic aerosols in Beijing, China: Insights from saccharides and n-alkanes,
436 *Environ. Pollut.*, 243, 1579-1587, doi: 10.1016/j.envpol.2018.09.118, 2016.

437 Kang, M., Kim, K., Choi, N., Kim, Y. P., and Lee, J. Y.: Recent Occurrence of PAHs and n-Alkanes in PM_{2.5} in Seoul,
438 Korea and Characteristics of Their Sources and Toxicity, *Int. J. Environ. Res. Public Health*, 17, 1397, doi:
439 10.3390/ijerph17041397, 2020.

440 Kavouras, I. G, Koutrakis, P., Tsapakis, M., Lagoudaki, E., Stephanou, E. G, Baer, D. V., and Oyola, P.: Source
441 apportionment of urban particulate aliphatic and polynuclear aromatic hydrocarbons (PAHs) using multivariate methods,
442 *Environ. Sci. Technol.*, 35, 2288-2294, doi: 10.1021/es001540z, 2001.

443 Kawamura, K., Ishimura, Y., and Yamazaki, K.: Four years' observations of terrestrial lipid class compounds in marine
444 aerosols from the western North Pacific, *Global Biogeochem Cycles*, 17, 1-19, doi: 10.1029/2001GB001810, 2003.

445 Li, F. X., Gu, J. W., Xin, J. Y., Schnelle-Kreis, J., Wang, Y. S., Liu, Z. R., Shen, R. R., Michalke, B., Abbaszade, G., and
446 Zimmermann, R.: Characteristics of chemical profile, sources and PAH toxicity of PM_{2.5} in Beijing in autumn-winter transit
447 season with regard to domestic heating, pollution control measures and meteorology, *Chemosphere*, 276, doi:
448 10.1016/j.chemosphere.2021.130143, 2021.

449 Li, W. F., Peng, Y., and Bai, Z. P.: Distributions and sources of n-alkanes in PM_{2.5} at urban, industrial and coastal sites in
450 Tianjin, China, *J. Environ. Sci. (China)*, 22, 1551-1557, doi: 10.1016/S1001-0742(09)60288-6, 2010.

451 Li, X. R., Wang, Y. S., Guo, X. Q., and Wang, Y. F.: Seasonal variation and source apportionment of organic and inorganic
452 compounds in PM_{2.5} and PM₁₀ particulates in Beijing, China, *J. Environ. Sci. (China)*, 25, 741-750, doi: 10.1016/S1001-
453 0742(12)60121-1, 2013.

454 Li, Y. S., Cao, J. J., Li, J. J., Zhou, J. M., Xu, H. M., Zhang, R. J., and Ouyang, Z. Y.: Molecular distribution and seasonal
455 variation of hydrocarbons in PM_{2.5} from Beijing during 2006, *Particuology*, 11, 78-85, doi: 10.1016/j.partic.2012.09.002,
456 2013.

457 Liao, H. T., Lee, C. L., Tsai, W. C., Yu, J. Z., Tsai, S. W., Chou, C. C K, and Wu, C. F.: Source apportionment of urban
458 PM_{2.5} using positive matrix factorization with vertically distributed measurements of trace elements and nonpolar organic
459 compounds, *Atmos. Pollut. Res.*, 12, 200-207, doi: 10.1016/j.apr.2021.03.007, 2021.

460 Liu, L. Y., Wei, G. L., Wang, J. Z., Guan, Y. F., Wong, C. S, Wu, F. C., and Zeng, E. Y: Anthropogenic activities have
461 contributed moderately to increased inputs of organic materials in marginal seas off China, *Environ. Sci. Technol.*, 47,
462 11414-11422, doi: 10.1021/es401751k, 2013.

463 Liu, X. D., Meng, J. J., Hou, Z. F., Yi, Y. N., Wei, B. J., and Fu, M. X.: Pollution Characteristics and Source Analysis of n-
464 alkanes and Saccharides in PM_{2.5} During the Winter in Liaocheng City, *Environ. Sci. (in Chinese)*, 40, 548-557, doi:
465 10.13227/j.hjcx.201807132, 2019.

466 Lv, L. L., Chen, Y. J., Han, Y., Cui, M., Wei, P., Zheng, M., and Hu, J. N.: High-time-resolution PM_{2.5} source apportionment
467 based on multi-model with organic tracers in Beijing during haze episodes, *Sci. Total Environ.*, 772, 144766, doi:
468 10.1016/j.scitotenv.2020.144766, 2020.

469 Lyu, R. H., Shi, Z. B., Alam, M. S., Wu, X. F., Liu, D., Vu, T. V, Stark, C., Xu, R. X., Fu, P. Q., Feng, Y. C., and Harrison, R.
470 M: Alkanes and aliphatic carbonyl compounds in wintertime PM 2.5 in Beijing, China, *Atmos. Environ.*, 202, 244-255, doi:
471 10.1016/j.atmosenv.2019.01.023, 2019.

472 Lyu, Y., Xu, T. T., Yang, X., Chen, J. M., Cheng, T. T., and Li, X.: Seasonal contributions to size-resolved n-alkanes (C8-
473 C40) in the Shanghai atmosphere from regional anthropogenic activities and terrestrial plant waxes, *Sci. Total Environ.*, 579,
474 1918-1928, doi: 10.1016/j.scitotenv.2016.11.201, 2016.

475 Ma, J. Z., Xu, X. B., Zhao, C. S., and Yan, P.: A review of atmospheric chemistry research in China: Photochemical smog,
476 haze pollution, and gas-aerosol interactions, *Adv. Atmos. Sci.*, 29, 1006-1026, doi: 10.1007/s00376-012-1188-7, 2012.

477 Marzi, R., Torkelson, B. E., and Olson, R. K.: A revised carbon preference index, *Org. Geochem.*, 20, 1303-1306, doi:
478 10.1016/0146-6380(93)90016-5, 1993.

479 Michoud, V., Kukui, A., Camredon, M., Colomb, A., Bordon, A., Miet, K., Aumont, B., Beekmann, M., Durand-Jolibois, R.,
480 Perrier, S., Zapf, P., Siour, G., Ait-Helal, w., Locoge, N., Sauvage, S., Afif, C., Gros, V., Furger, M., Ancellet, G., and
481 Doussin, J. F.: Radical budget analysis in a suburban European site during the MEGAPOLI summer field campaign, *Atmos.*
482 *Chem. Phys.*, 12, 11951-11974, doi: 10.5194/acp-12-11951-2012, 2012.

483 Moeinaddini, M., Sari, A. E., Bakhtiari, A. R., Chan, A. Y. C., Taghavi, S. M., Hawker, D., and Connell, D.: Source
484 apportionment of PAHs and n-alkanes in respirable particles in Tehran, Iran by wind sector and vertical profile, *Environ. Sci.*
485 *Pollut. Res.*, 21, 7757-7772, doi: 10.1007/s11356-014-2694-1, 2014.

486 Niu, H. Y., Zhao, X., Dai, Z. X., Wang, G. H., and Wang, L. S.: Characterization, source apportionment of particulate matter
487 and n-alkanes in atmospheric aerosols in Nanjing City, *Environ. pollut. Control (in Chinese)*, 27, 363-366, doi:
488 10.1007/s10971-005-6694-y, 2005.

489 Oros, D. R., and Simoneit, B. R. T.: Identification and emission rates of molecular tracers in coal smoke particulate matter,
490 *Fuel*, 79, 515-536, doi: 10.1016/S0016-2361(99)00153-2, 2000.

491 Presto, A. A., Miracolo, M. A., Kroll, J. H., Worsnop, D. R., Robinson, A. L., and Donahue, N. M.: Intermediate-volatility
492 organic compounds: a potential source of ambient oxidized organic aerosol, *Environ. Sci. Technol.*, 43, 4744-4749, doi:
493 10.1021/es803219q, 2009.

494 Qi, M. X., Jiang, L., Liu, Y. X., Xiong, Q. L., Sun, C. Y., Li, X., Zhao, W. J., and Yang, X. C.: Analysis of the Characteristics
495 and Sources of Carbonaceous Aerosols in PM_{2.5} in the Beijing, Tianjin, and Langfang Region, China, *Int. J. Environ. Res.*
496 *Public Health*, 15, 1438, doi: 10.3390/ijerph15071483, 2018.

497 Ren, L. J., Fu, P. Q., He, Y., Hou, J. Z., Chen, J., Pavuluri, C. M., Sun, Y. L., and Wang, Z. F.: Molecular distributions and
498 compound-specific stable carbon isotopic compositions of lipids in wintertime aerosols from Beijing, *Sci. Rep.*, 6, 27481,
499 doi: 10.1038/srep27481, 2016.

500 Ren, L. J., Hu, W., Hou, J. Z., Li, L. J., Yue, S. Y., Sun, Y. L., Wang, Z. F., Li, X. F., Pavuluri, C. M., Hou, S. J., Liu, C. Q.,
501 Kawamura, K., Ellam, R. M., and Fu, P. Q.: Compound-Specific Stable Carbon Isotope Ratios of Terrestrial Biomarkers in
502 Urban Aerosols from Beijing, China, *ACS Earth Space Chem.*, 3, 1896-1904, doi: 10.1021/acsearthspacechem.9b00113,
503 2019.

504 Ren, Y. Q., Wang, G. H., Wu, C., Wang, J. Y., Li, J. J., Zhang, L., Han, Y. N., Liu, L., Cao, C., Cao, J. J., He, Q., and Liu, X.
505 C.: Changes in concentration, composition and source contribution of atmospheric organic aerosols by shifting coal to
506 natural gas in Urumqi, *Atmos. Environ.*, 148, 306-315, doi: 10.1016/j.atmosenv.2016.10.053, 2017.

507 Rogge, W. F., Hildemann, L. M., Mazurek, M. A., Cass, G. R., and Simoneit, B. R. T.: Sources of fine organic aerosol. 4.
508 Particulate abrasion products from leaf surfaces of urban plants, *Environ. Sci. Technol.*, 27, 2700-2711, doi:
509 10.1021/es00049a008, 1993.

510 Schauer, J. J., Kleeman, M. J., Cass, G. R., and Simoneit, B. R. T.: Measurement of Emissions from Air Pollution Sources. 5.
511 C1-C32 Organic Compounds from gasoline-Powered Motor Vehicles, *Environ. Sci. Technol.*, 36, 1169-1180, doi:
512 10.1021/es0108077, 2002.

513 Simoneit, B. R. T.: Application of Molecular Marker Analysis to Vehicular Exhaust for Source Reconciliations, *Int. J. Environ.*
514 *Anal. Chem.*, 22, 203-232, doi: 10.1080/03067318508076422, 1985.

515 Simoneit, B. R T: Organic matter of the troposphere - V: Application of molecular marker analysis to biogenic emissions into
516 the troposphere for source reconciliations, *J. Atmos. Chem.*, 8, 251-275, doi: 10.1007/BF00051497, 1989.

517 Simoneit, B. R T, Kobayashi, M., Mochida, M., Kawamura, K., and Huebert, B. J: Aerosol particles collected on aircraft
518 flights over the northwestern Pacific region during the ACE-Asia campaign: composition and major sources of the organic
519 compounds, *J. Geophys. Res.*, 109, doi: 10.1029/2004JD004565, 2004.

520 Sun, N., Li, X. D., Ji, Y., Huang, H. Y., Ye, Z. L., and Zhao, Z. Z.: Sources of PM_{2.5}-Associated PAHs and n-alkanes in
521 Changzhou China, *Atmosphere*, 12, 1127, doi: 10.3390/atmos12091127, 2021.

522 Tang, G. Q., Zhang, J. Q., Zhu, X. W., Song, T., and Wang, Y. S.: Mixing layer height and its implications for air pollution
523 over Beijing, China, *Atmospheric Chem. Phys.*, 16, 2459-2475, doi: 10.5194/acpd-15-28249-2015, 2016.

524 US EPA: EPA Positive Matrix Factorization (PMF) 5.0 Fundamentals and User Guide. EPA/600/R-14/108, EPA, Washington,
525 DC, 2014.

526 Wagner, P., and Schäfer, K.: Influence of mixing layer height on air pollutant concentrations in an urban street canyon, *Urban*
527 *Clim.*, 22, 64-79, doi: 10.1016/j.uclim.2015.11.001, 2017.

528 Wang, F. W., Guo, Z. G., Lin, T., and Rose, N. L: Seasonal variation of carbonaceous pollutants in PM_{2.5} at an urban
529 'supersite' in Shanghai, China, *Chemosphere*, 146, 238-244, doi: 10.1016/j.chemosphere.2015.12.036, 2016.

530 Wang, G. H., and Kawamura, K.: Molecular characteristics of urban organic aerosols from Nanjing: a case study of a mega-
531 city in China, *Environ. Sci. Technol.*, 39, 7430-7438, doi: 10.1021/es051055+, 2005.

532 Wang, G. H., Kawamura, K., Lee, S. C., Ho, K. F., and Cao, J. J.: Molecular, Seasonal, and Spatial Distributions of Organic
533 Aerosols from Fourteen Chinese Cities, *Environ. Sci. Technol.*, 40, 4619-4625, doi: 10.1021/es060291x, 2006.

534 Wang, G. H., Huang, L. M., Zhao, X., Niu, H. Y., and Dai, Z. X.: Aliphatic and polycyclic aromatic hydrocarbons of
535 atmospheric aerosols in five locations of Nanjing urban area, China, *Atmos. Res.*, 81, 54-66, doi:
536 10.1016/j.atmosres.2005.11.004, 2006.

537 Wang, G. H., Zhang, R. Y., Gomez, M. E, Yang, L. X., Zamora, M. L., Hu, M., Lin, Y., Peng, J. F., Guo, S., Meng, J. J., Li, J.
538 J., Chen, C. L., Hu, T. F., Ren, Y. Q., Wang, Y. S., Gao, J., Cao, J. J., An, Z. S., Zhou, W. J., Li, G. H., Wang, J. Y., Tian, P. F.,
539 Marrero-Ortiz, W., Secrest, J., Du, Z. F., Zheng, J., Shang, D. J., Zheng, L. M., Shao, M., Wang, W. G., Huang, Y., Wang, Y.,
540 Zhu, Y. J., Li, Y. X., Hu, J. X., Pan, B. W., Cai, L., Cheng, Y. T., Ji, Y. M., Zhang, F., Rosenfeld, D., Liss, P. S, Duce, R. A,
541 Kolb, C. E, and Molina, M. J: Persistent sulfate formation from London Fog to China haze, *P. Natl. Acad. Sci. USA*, 113,
542 13630-13635, doi: 10.1073/pnas.1616540113, 2016.

543 Wang, H. F., Li, Z. Q., Lv, Y., Zhang, Y., Xu, H., Guo, J. P., and Goloub, P.: Determination and climatology of the diurnal
544 cycle of the atmospheric mixing layer height over Beijing 2013–2018: lidar measurements and implications for air pollution,
545 *Atmospheric Chem. Phys.*, 20, 8839-8854, doi: 10.5194/acp-20-8839-2020, 2020.

546 Wang, J. Z., Ho, S. S. H., Ma, S. X., Cao, J. J., Dai, W. T., Liu, S. X., Shen, Z. X., Huang, R. J., Wang, G. H., and Han, Y. M.:
547 Carbonaceous species in PM_{2.5} and PM₁₀ in urban area of Zhengzhou in China: Seasonal variations and source
548 apportionment, *Sci. Total Environ.*, 550, 961-971, doi: 10.1016/j.scitotenv.2016.01.138, 2016.

549 Wang, Q., Jiang, N., Yin, S. S., Li, X., Yu, F., Guo, Y., and Zhang, R. Q.: Carbonaceous species in PM_{2.5} and PM₁₀ in urban
550 area of Zhengzhou in China: Seasonal variations and source apportionment, *Atmos. Res.*, 191, 1-11, doi:
551 10.1016/j.atmosres.2017.02.003, 2017.

552 Wei, M., Li, M. Y., Xu, C. H., Xu, P. J., and Liu, H. F.: Pollution characteristics of bioaerosols in PM_{2.5} during the winter
553 heating season in a coastal city of northern China, *Environ. Sci. Pollut. Res.*, 27, 27750-27761, doi: 10.1007/s11356-020-
554 09070-y, 2020.

555 Wick, C. D, Siepmann, J., Klotz, W. L, and Schure, M. R.: Temperature effects on the retention of n-alkanes and arenes in
556 helium–squalane gas–liquid chromatography: experiment and molecular simulation, *J. Chromatogr. A*, 957, 181-190, doi:

557 10.1016/S0021-9673(02)00171-1, 2002.

558 Xu, H. M., Tao, J., Ho, S. S. H., Ho, K. F., Cao, J. J., Li, N., Chow, J. C., Wang, G. H., Han, Y. M., and Zhang, R. J.:
559 Characteristics of fine particulate non-polar organic compounds in Guangzhou during the 16th Asian Games: Effectiveness
560 of air pollution controls, *Atmos. Environ.*, 76, 94-101, doi: 10.1016/j.atmosenv.2012.12.037, 2013.

561 Xu, T. T., Lv, Y., Cheng, T. T., and Li, X.: Using comprehensive GC×GC to study PAHs and n-alkanes associated with
562 PM_{2.5} in urban atmosphere, *Environ. Sci. Pollut. Res.*, 22, 5253-5262, doi: 10.1007/s11356-014-3695-9, 2015.

563 Yadav, S., Tandon, A., and Attri, A., Monthly and seasonal variation in aerosol associated n-alkane profiles in relation to
564 meteorological parameters in New Delhi, India, *Aerosol Air Qual. Res.*, 13, 287-300, doi: 10.4209/aaqr.2012.01.0004, 2013.

565 Yang, X. H., Luo, F. X., Li, J. Q., Chen, D. Y., E, Y., Lin, W. L., and Jin, J.: Alkyl and aromatic nitrates in atmospheric
566 particles determined by gas chromatography tandem mass spectrometry, *J. Am. Soc. Mass Spectrom.*, 30, 2762-2770, doi:
567 10.1007/s13361-019-02347-8, 2019.

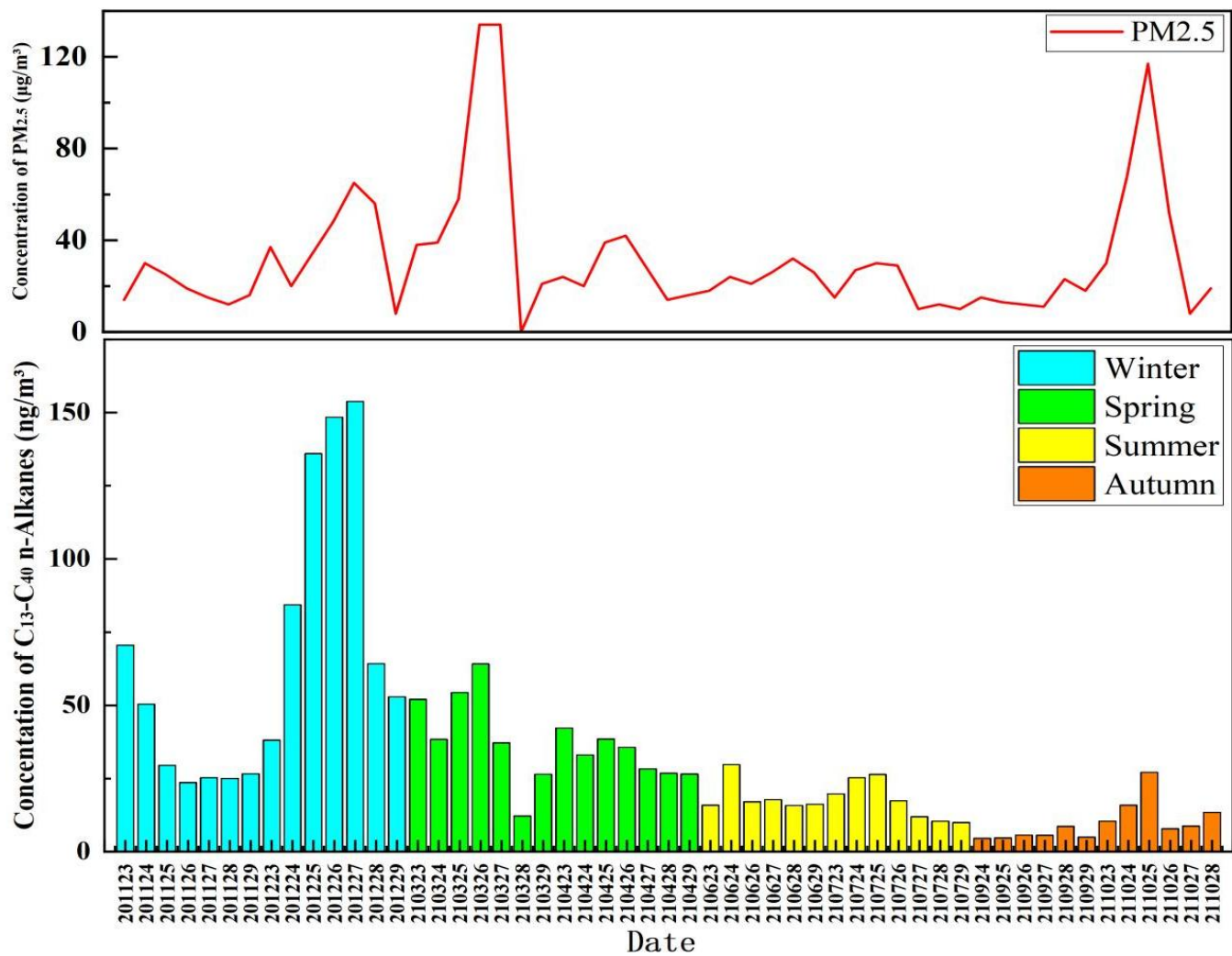
568 Yao, L., Li, X. R., Guo, X. Q., Liu, X. R., and Wang, Y. S.: Pollution Characteristics of n-alkanes in Atmospheric Fine
569 Particles During Spring Festival of 2007 in Beijing, *Environ. Sci.* (in Chinese), 30, 589-593, doi:
570 10.13227/j.hjlx.2009.02.042, 2009.

571 Yuan, J. W., Liu, G., Li, J. H., and Xu, H.: Chemical Composition of Alkanes and Organic Acids in Vehicle Exhaust, *Environ.*
572 *Sci.* (in Chinese), 37, 2052-2058, doi: 10.13227/j.hjlx.2016.06.007, 2016.

573 Zhao, Y., Zhang, Y., Fu, P., Ho, S. S., Ho, K. F., Liu, F., Zou, S., Wang, S., and Lai, S.: Non-polar organic compounds in
574 marine aerosols over the northern South China Sea: Influence of continental outflow, *Chemosphere*, 153, 332–339, doi:
575 10.1016/j.chemosphere.2016.03.069, 2016.

576 Zhang, R. Y., Wang, G. H., Guo, S., Zamora, M. L., Ying, Q., Lin, Y., Wang, W. G., Hu, M., and Wang, Y.: Formation of
577 urban fine particulate matter, *Chem. Rev.*, 115, 3803-3855, doi: 10.1021/acs.chemrev.5b00067, 2015.

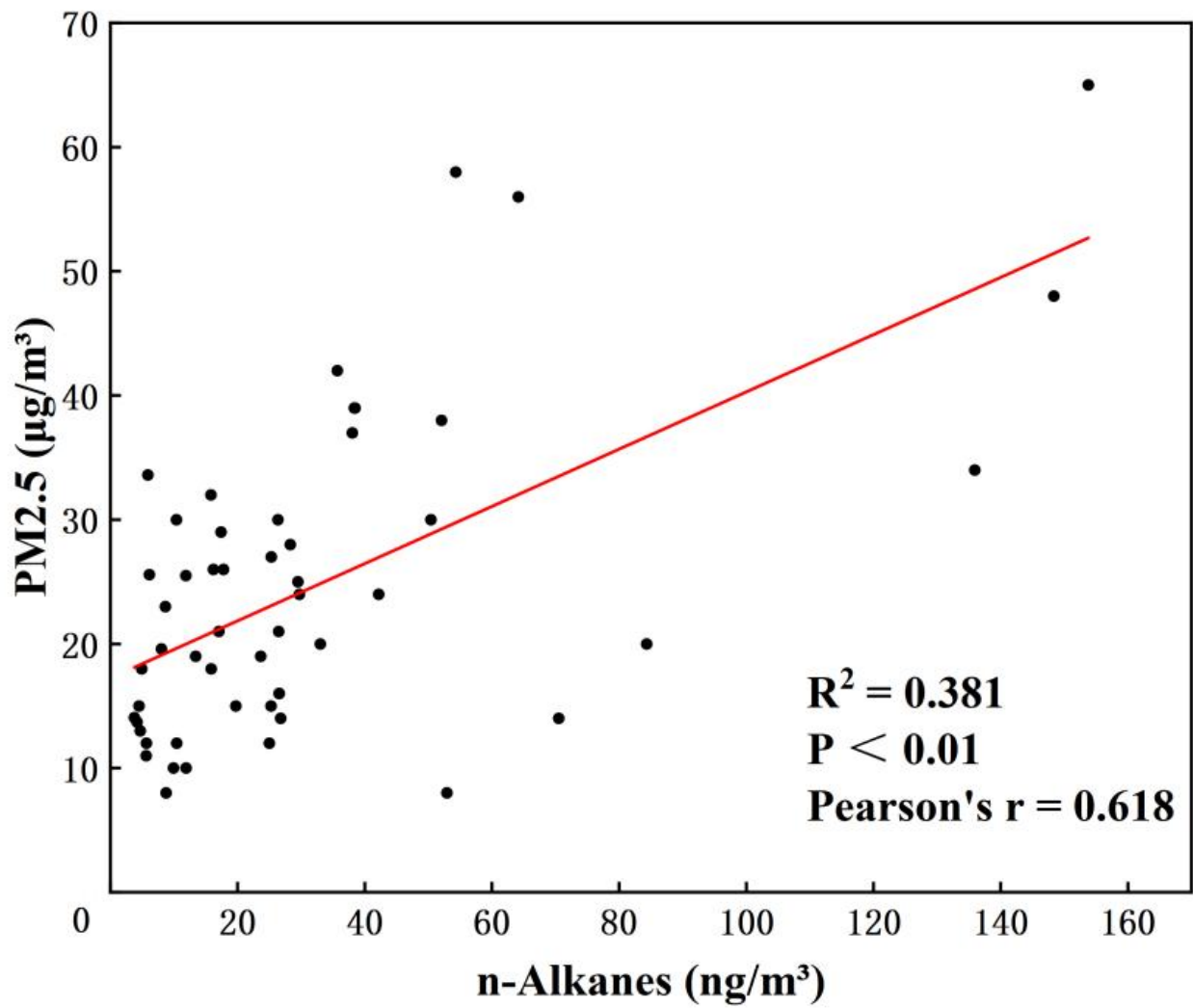
578 Zhu, X. L., Zhang, Y. H., Zeng, L. M., and Wang, W.: Source Identification of Ambient PM_{2.5} in Beijing, *Res. Environ. Sci.*
579 (in Chinese), 18, 1-5, doi: 10.1007/s10971-005-6694-y, 2005.



580

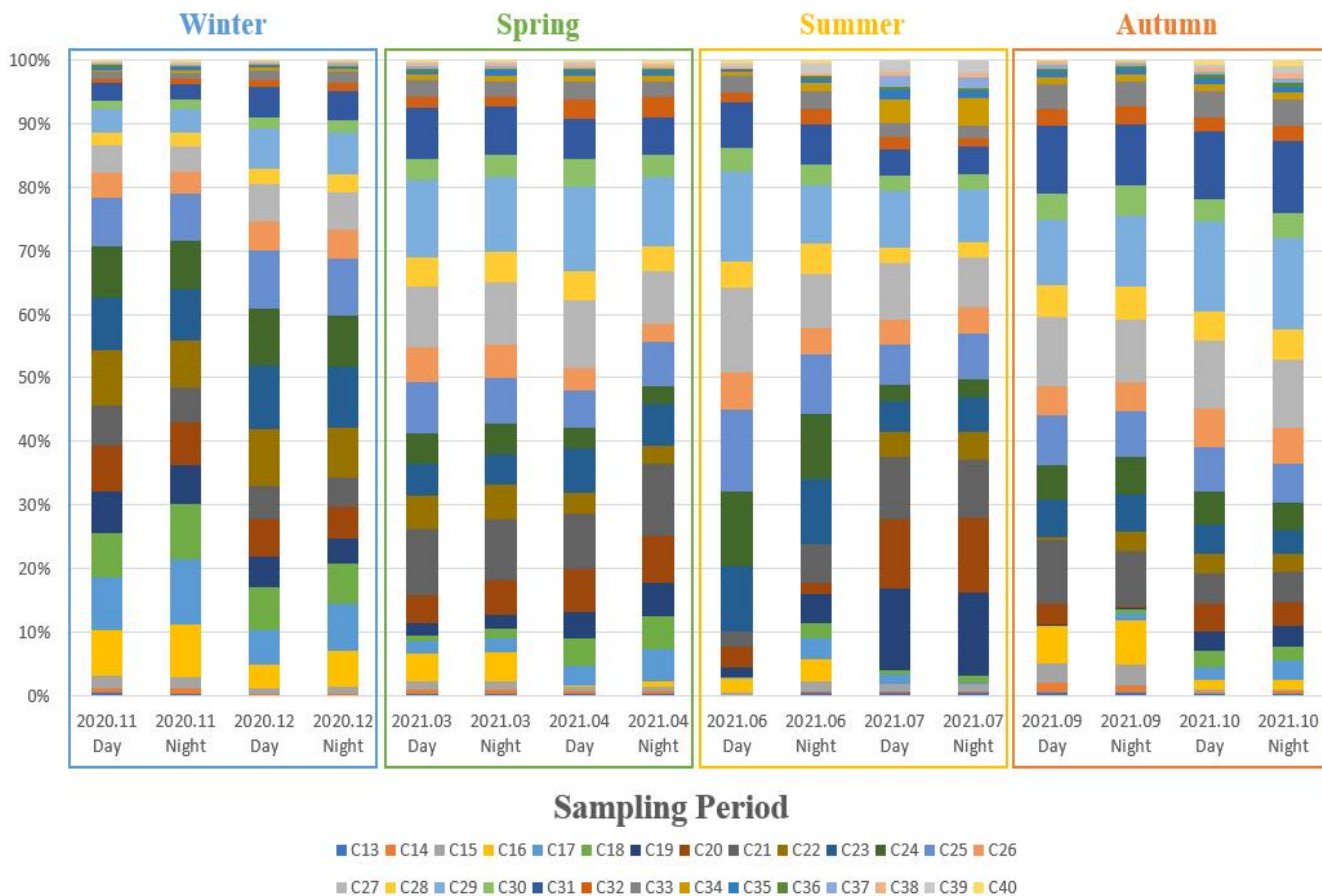
581 **Figure 1. Temporal variations in PM_{2.5} and particulate-bound *n*-alkane concentrations during the sampling period in Beijing.**

582 **(The concentrations of C₁₃-C₄₀ *n*-Alkanes and PM_{2.5} are the average of the day and night).**



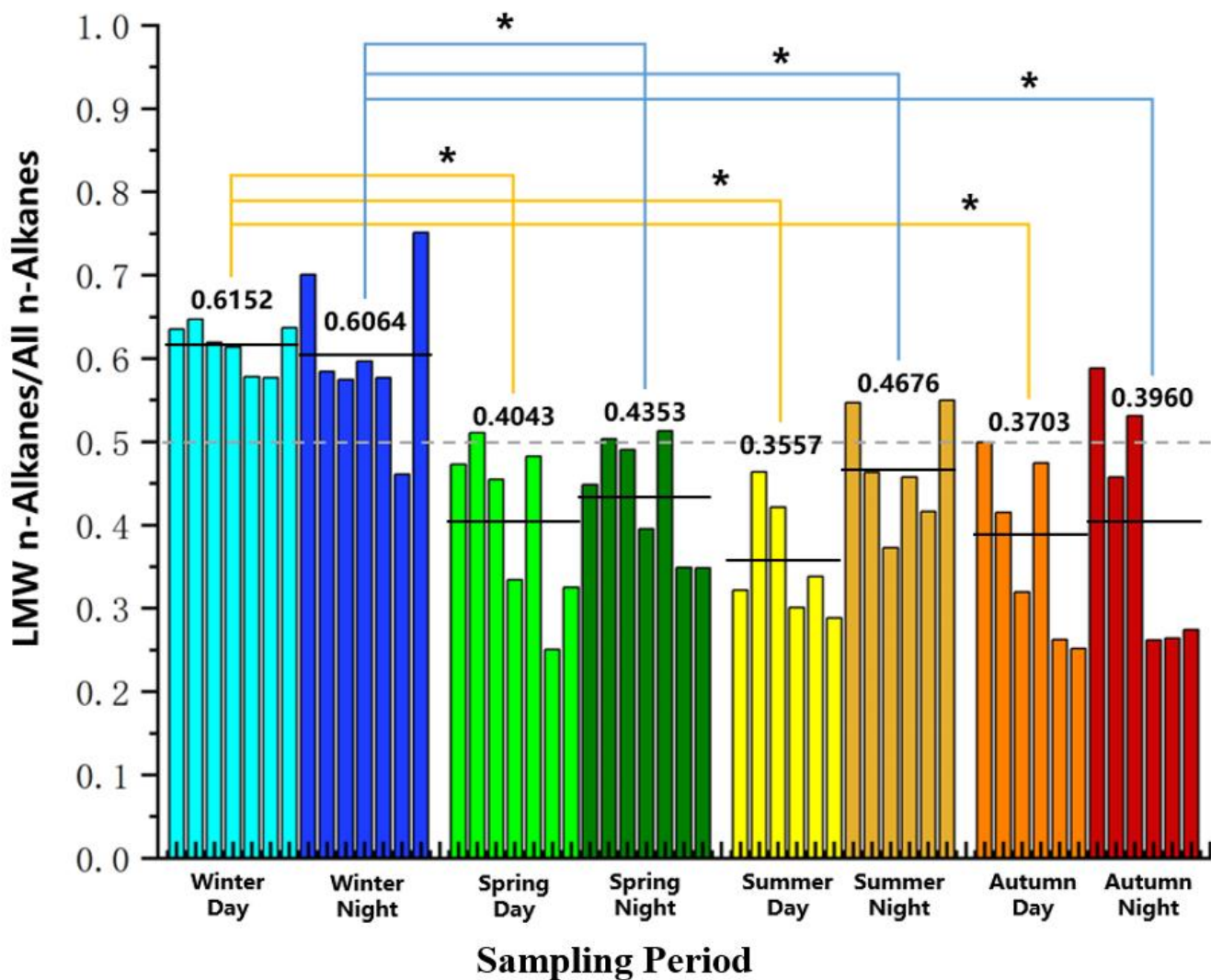
583

584 Figure 2. Association between particulate-bound *n*-alkanes and PM2.5 in Beijing.



585

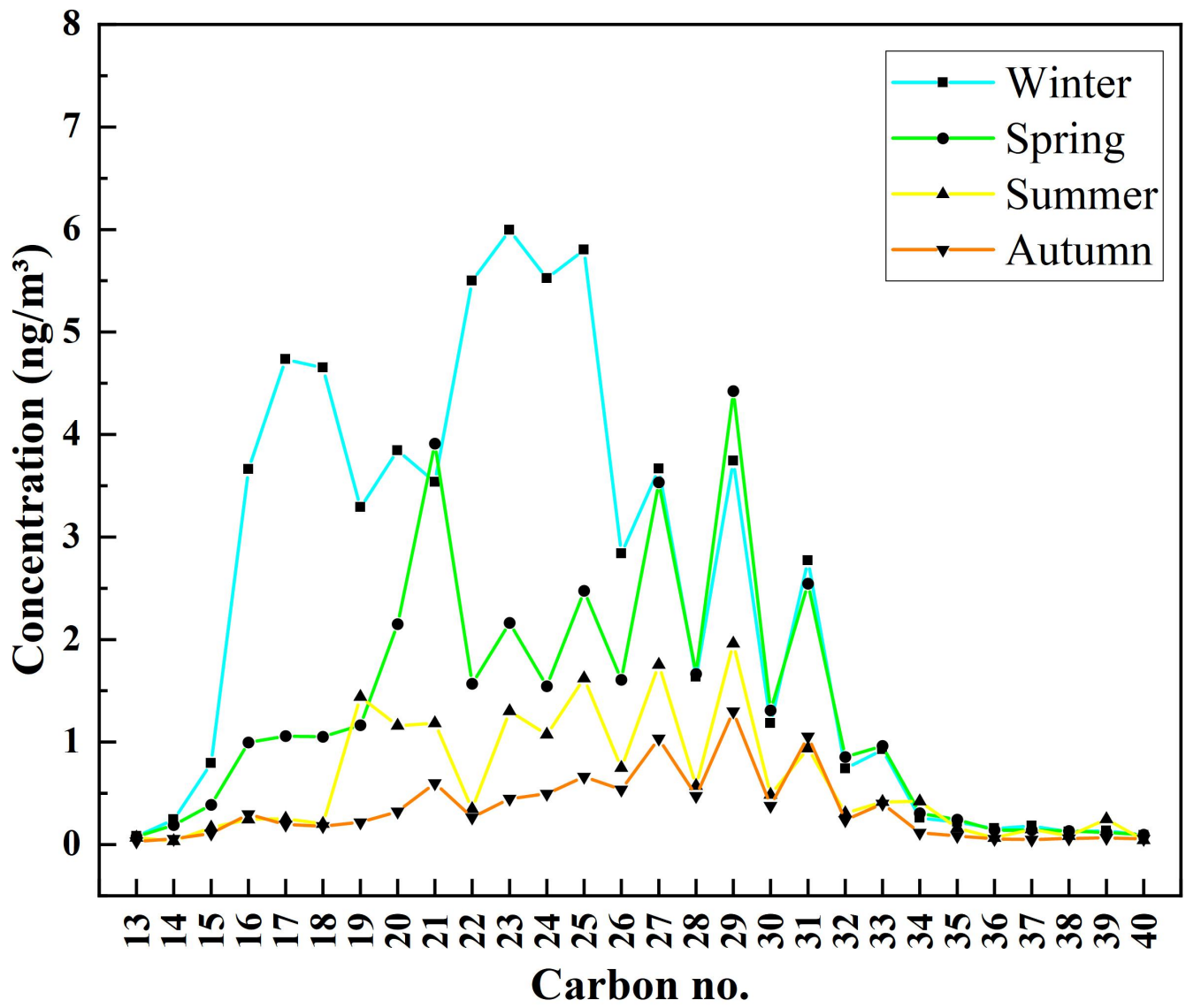
586 **Figure 3. Contributions of particulate-bound *n*-alkane homologs to the total *n*-alkane concentrations in the day and night samples**
 587 **in the different seasons of Beijing.**



588

589 Figure 4. Contributions of low molecular weight *n*-alkanes in the day and night samples in the different seasons of Beijing.

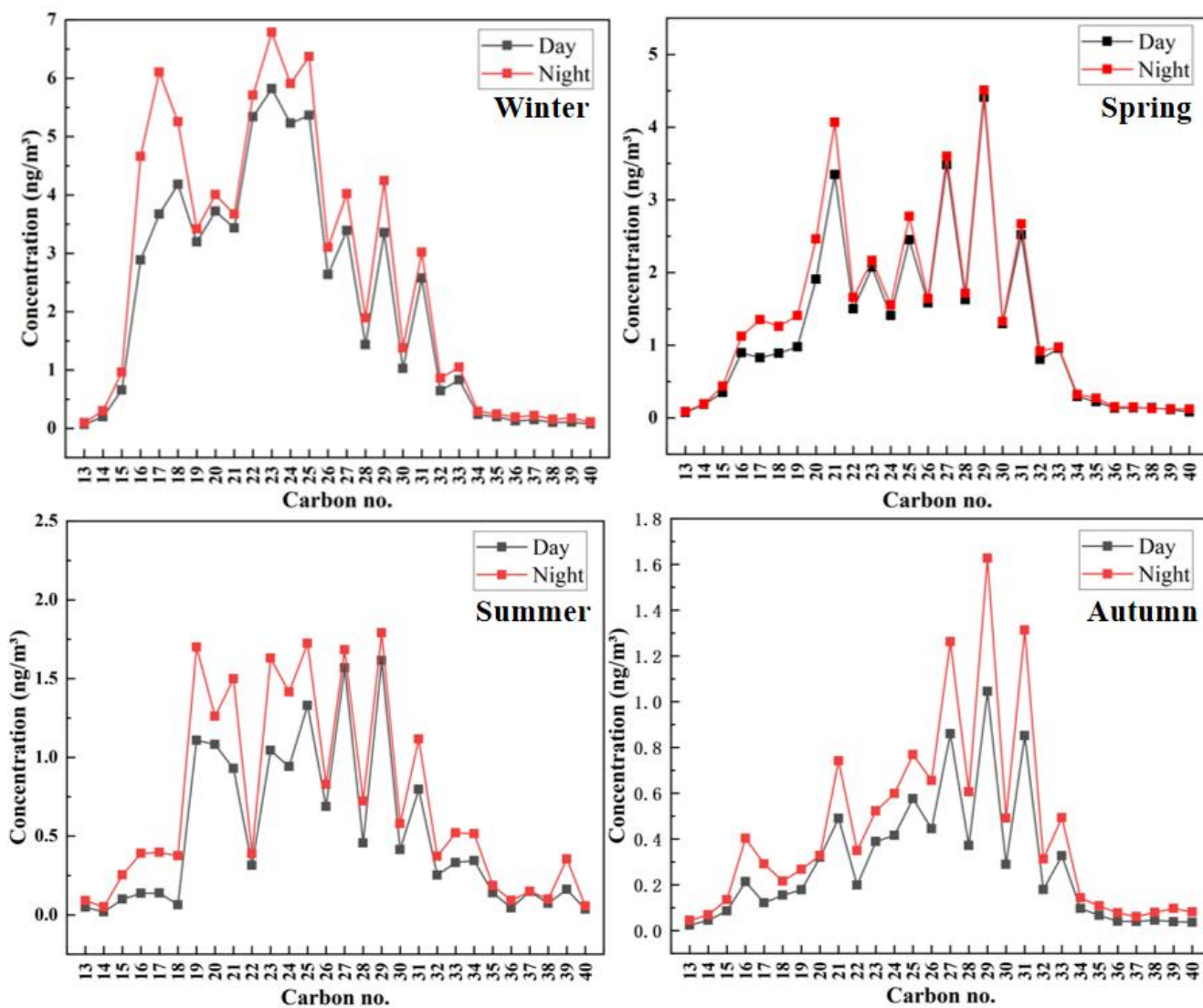
590 (* indicates a significant difference, the dashed line represents the 50% percentage, the solid line shows the average proportion of
 591 LMW *n*-alkanes).



592

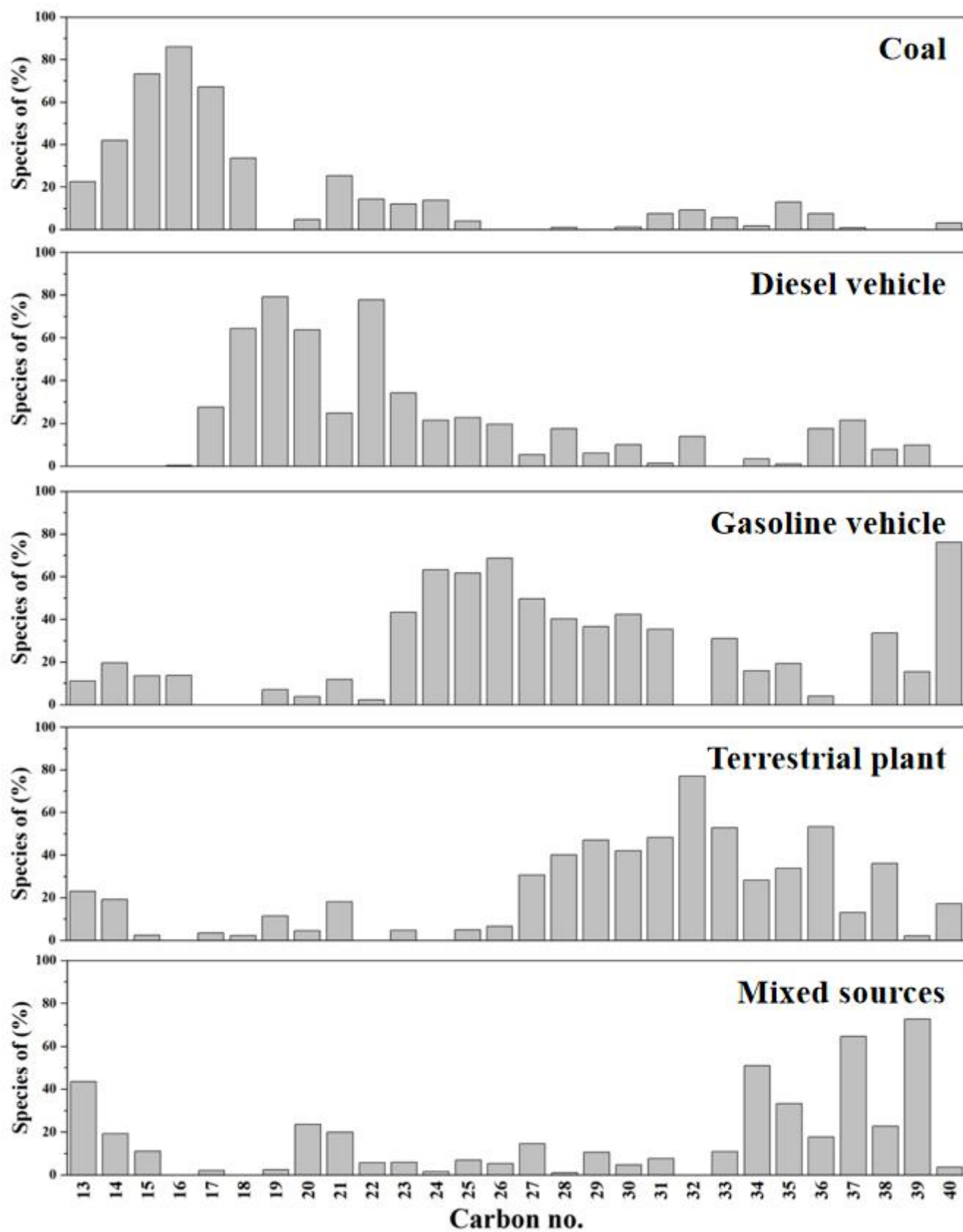
593

Figure 5. Average concentration distributions of the particulate-bound *n*-alkane homologs in the different seasons of Beijing.



594

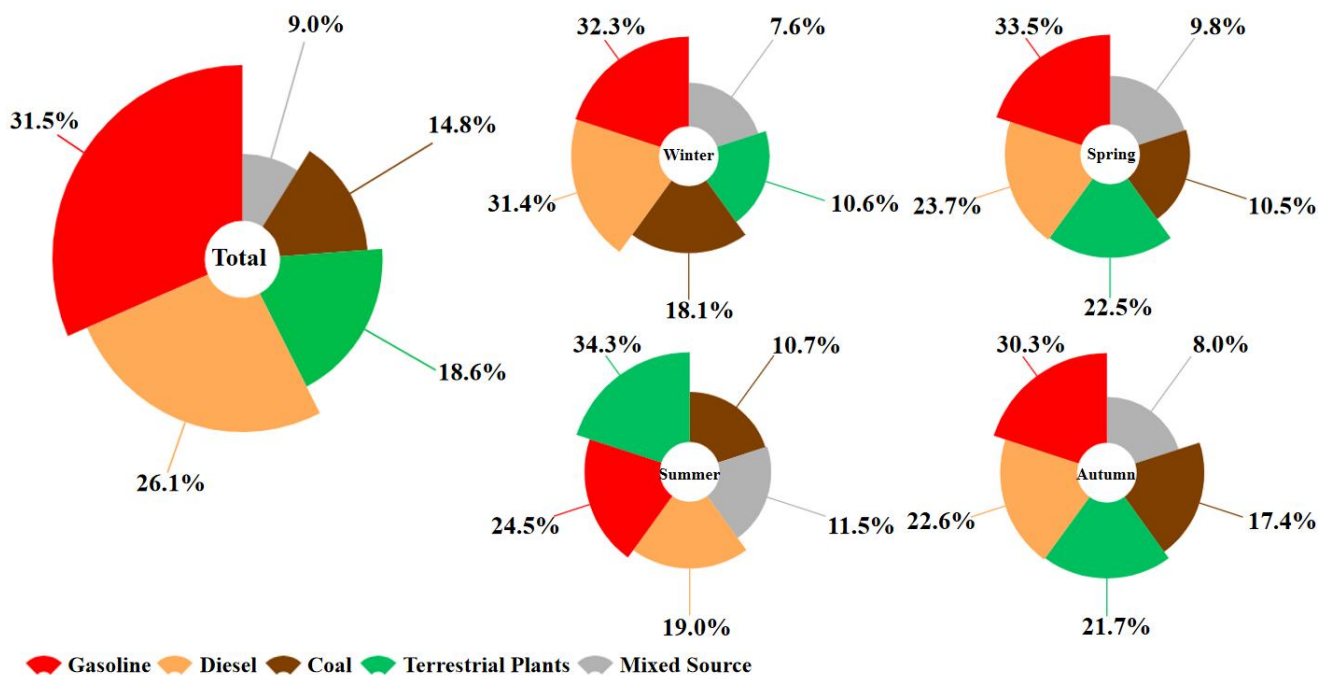
595 Figure 6. Concentration distributions of the particulate-bound *n*-alkane homologs in the day and night in the different seasons of
 596 Beijing.



597

598

Figure 7. Proportions of the different *n*-alkane homologs in the factors identified by the positive matrix factorization model.



599
600 **Figure 8. Sources and contributions of particulate-bound *n*-alkanes in Beijing.**

601 **Table 1. PM2.5 and particulate-bound *n*-alkane concentrations in different seasons in Beijing.**

Species	Winter ^a		Spring ^b		Summer ^c		Fall ^d	
	Mean	Range	Mean	Range	Mean	Range	Mean	Range
PM2.5 ($\mu\text{g}/\text{m}^3$)	28.5	8.00–65.0	43.5	0–134	21.5	10.0–32.0	32.2	8.00–117
<i>n</i> -Alkanes (ng/m^3)	66.3	17.1–89.9	36.8	12.2–64.1	18.0	9.92–29.7	9.78	4.51–27.1

602 ^a Winter: November and December in 2020;

603 ^b Spring: March and April in 2021;

604 ^c Summer: June and July in 2021;

605 ^d Fall: September and October in 2021.

606 **Table 2. Source indices for particulate-bound *n*-alkane in Beijing.**

Source Index	Winter		Spring		Summer		Fall	
	Day	Night	Day	Night	Day	Night	Day	Night
Cmax^a	C23	C23	C29	C29	C29	C29	C29	C29
CPI^b	1.16	1.18	1.85	1.76	2.15	1.87	1.90	1.78
WNA%^c	17.4	18.5	35.0	33.1	43.0	39.2	39.6	35.1
PNA%^d	82.6	81.5	65.0	66.9	57.0	60.8	60.5	64.9

607 ^a Cmax: Carbon maximum number;

608 ^b CPI: Carbon preference index;

609 ^c WNA%: Plant wax *n*-alkane ratio;

610 ^d PNA%: Petrogenic *n*-alkane ratio.